Journal of South American Earth Sciences 19 (2005) 155–171

Journal of
South American
Earth Sciences

www.elsevier.com/locate/jsames

A Late Proterozoic–Early Paleozoic magmatic cycle in Sierra de la Ventana, Argentina

D.A. Gregori[a,*], V.L. López[a], L.E. Grecco[b]

[a]Departamento de Geología, CONICET and Cátedra de Geología Argentina, Universidad Nacional del Sur, San Juan 670, 8000 Bahía Blanca, Argentina
[b]Departamento de Geología, CONICET and Cátedra de Geoquímica, Universidad Nacional del Sur, San Juan 670, 8000 Bahía Blanca, Argentina

Received 1 May 2003; accepted 1 October 2004

Abstract

Late Proterozoic–Early Paleozoic intrusive and volcanic rocks of Sierra de la Ventana can be grouped into two magmatic assemblages: the Meyer and Cochenleufú suites. The older (700–570 Ma) is composed of S-type quartz-monzodiorites, synogranites, and monzogranites associated with andesites and rhyolites and related to volcanic-arc and postcollisional settings. The younger (540–470 Ma) corresponds to highly fractionated homogeneous A-type monzogranites, linked to final plutonic events during postorogenic extension in collisional belts. Strong similarities between Sierra de la Ventana magmatic rocks and the S- and A-type granites of the Cape granite suite in South Africa allow positive correlation. In both areas, primitive volcanic arcs or collisional orogens are recognized. Continuous transpressional shearing between the Swartland and Tygerberg terranes in the Saldania belt may have triggered the generation and emplacement of both suites.

Keywords: Argentina; Late proterozoic–Early paleozoic magmatism; Sierra de la ventana

1. Introduction

In southeastern Buenos Aires province, Argentina, Sierra de la Ventana is a 180 km long sigmoidal mountain belt, composed of basement and sedimentary cover (Fig. 1). The basement consists of Late Precambrian–Early Paleozoic deformed granites, rhyolites, and andesites. The Paleozoic sedimentary sequences can be divided into three groups. Conglomerates and quartzites compose the Curamalal (Ordovician–Silurian) and Ventana (Silurian–Devonian) Groups. The Pillahuincó Group (Upper Carboniferous–Permian) is composed of glacial deposits, black shales, and sandstones. Deformational episodes occurred during the Upper Devonian and Permian.

Keidel (1916) correlated the Sierra de la Ventana sequences with the Karoo Basin in South Africa, and Du Toit (1937) integrated both areas in the Samfrau Geosyncline. Andreis (1964), Andreis et al. (1989), Borrello (1962, 1964), Buggisch (1987), Harrington (1947, 1970, 1972, 1980), Iñiguez Rodríguez and Andreis (1971), Kilmurray (1968a,b, 1975), Kilmurray et al. (1985), Llambías and Prozzi (1975), Sellés Martínez (1989), Varela (1973, 1978), von Gosen et al. (1990, 1991), and von Gosen (2002), among others, carried out geological studies in Sierra de la Ventana. In addition, Grecco (1990), Grecco et al. (1984, 1999), Grecco and Gregori (1993), Varela et al. (1985), and Rapela and Pankhurst (2002) studied the petrography, geochemistry and geochronology, and reported preliminary geotectonic interpretations of the igneous rocks. Finally, Rapela et al. (2003) presented relevant data for understanding the tectonic setting of the Sierra de la Ventana granite.

In this paper, we present new petrographical and geochemical data about the intrusive and volcanic rocks of Sierra de la Ventana. These are integrated with regional geological data to postulate the magmatic source of the rocks and propose a model for the Late Proterozoic–Early Paleozoic tectonomagmatic evolution of this part of Gondwana.

* Corresponding author. Tel.: +54 291 4595101x3030; fax: +44 1604 716247.
E-mail address: usgregor@criba.edu.ar (D.A. Gregori).

0895-9811/$ - see front matter © 2005 Elsevier Ltd. All rights reserved.
doi:10.1016/j.jsames.2004.10.007

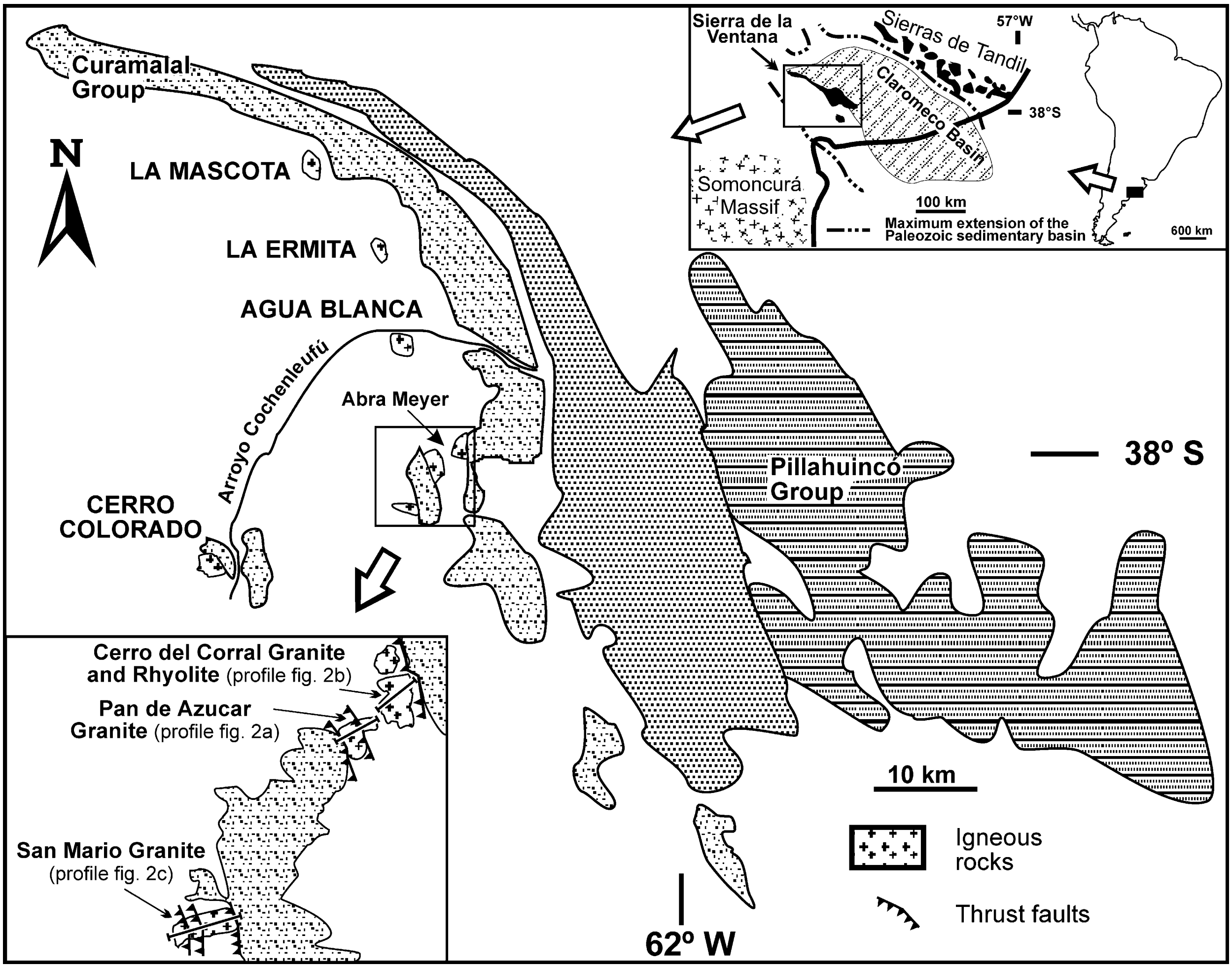

Fig. 1. Major tectonic domains in SE Buenos Aires. The box in the upper right-hand shows the location of Sierra de la Ventana, as expanded in the main area of the figure. The location of the studied igneous rocks is clarified in the lower left-hand box.

2. Field relationships and petrography of the igneous rocks

The igneous rocks crop out at La Mascota, La Ermita, Agua Blanca, Pan de Azucar, Cerro del Corral, San Mario, and Cerro Colorado (Fig. 1). Most are exposed on the western side of the Sierra de la Ventana due to tectonic transport to the northeast by thrust faults (Cobbold et al., 1986). The outcrops at Cerro Colorado, La Ermita, and Agua Blanca are granitic and rhyolitic rocks overlain by Quaternary sediments. The igneous rocks at San Mario, Pan de Azucar, and Cerro del Corral show tectonic contacts with the Paleozoic sedimentary cover (Fig. 1).

Field relationships in the San Mario, Pan de Azúcar, and Cerro del Corral granites, as well as in the Cerro del Corral rhyolite and Pan de Azúcar andesite, together with petrologic, structural, chemical, and geochronological data, suggest grouping these rocks as part of the Meyer suite. Most outcrops of the rocks are located near Abra Meyer. The Cochenleufú suite includes the Agua Blanca and Cerro Colorado granites and the La Ermita rhyolite, which outcrops near Arroyo Cochenleufú. They are slightly deformed and characterized by a distinctive magmatic fabric and chemical characteristics. This suite partially corresponds to the Sierra de la Ventana granite suite of Rapela et al. (2003).

2.1. Meyer suite

2.1.1. Cerro Pan de Azúcar

In Cerro Pan de Azúcar (Fig. 2a), the greenschists, metaquartzites, mafic bodies, and mylonitized granites (Pan de Azúcar Formation) described by Cuerda et al. (1975) underlie the Paleozoic sequence. Schiller (1930) and Cucchi (1966) inferred a tectonic contact, whereas von Gosen et al. (1990) found no evidence of intrusive contact. Cobbold et al. (1986) suggested a dextral overthrust to the northeast. Our interpretation is a NE-vergent overthrust suggested by the presence of ultramylonitic belts (344°/61°SW) in the granitic rocks.

As shown in Fig. 2a, the eastern flank of the Cerro Pan de Azucar consists of deformed plutonic and volcanic rocks.

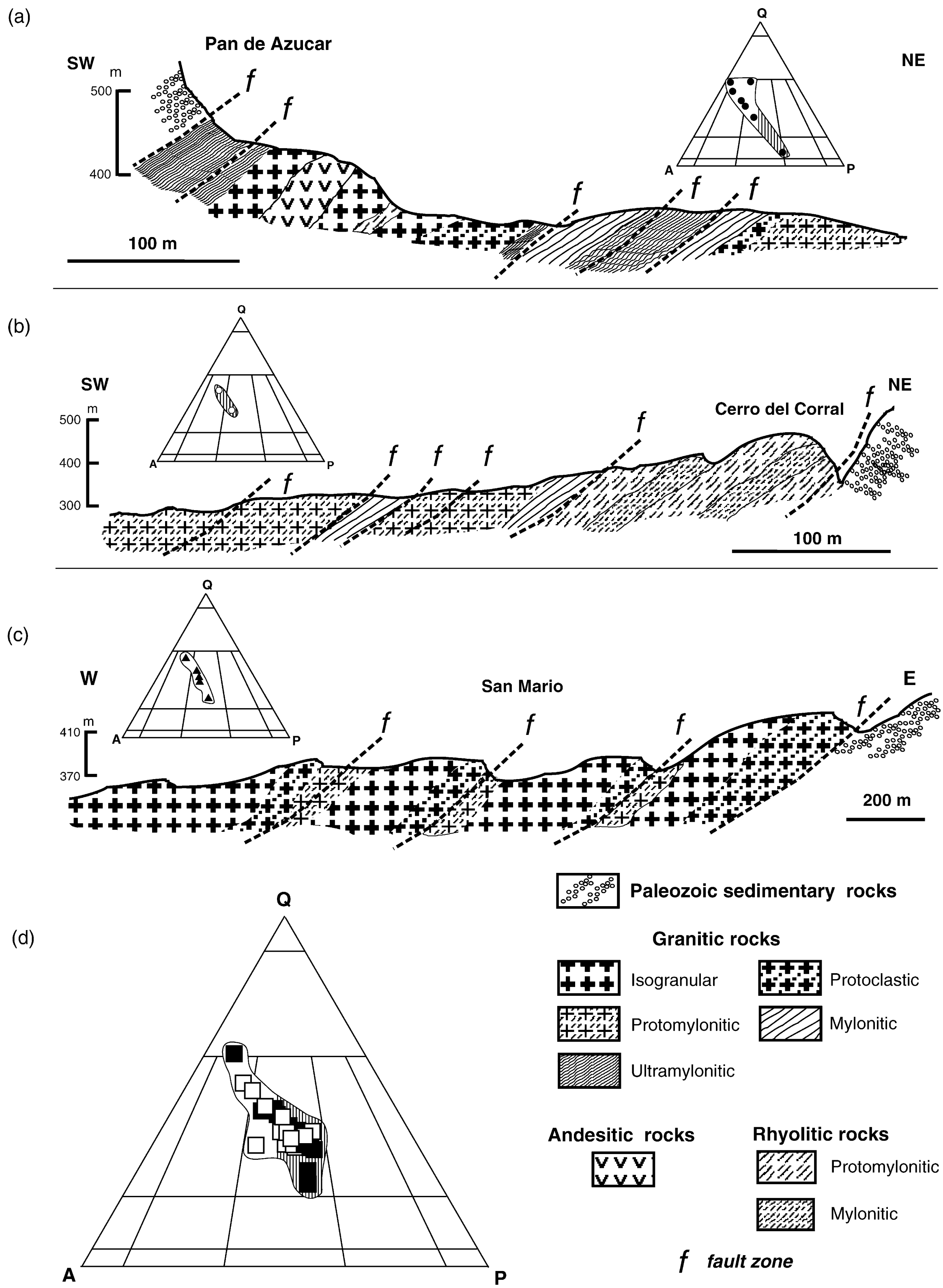

Fig. 2. Profiles at (a) Pan de Azucar, (b) Cerro del Corral, and (c) San Mario. (d) QAP diagram for the Cochenleufú suite.

Plutonic rocks exhibit isogranular to ultramylonitic textures. The former are composed of quartz, twinned K-feldspar, plagioclase ($An_{26–33}$), and biotite. Plagioclase is replaced by sericite, epidote, and calcite. In the QAP modal triangle (Fig. 2a), these rocks plot in the synogranite and monzogranite fields. In protoclastic and protomylonitic varieties, quartz, plagioclase, and K-feldspar were disrupted to produce porphyroclasts with patchy extinction and fracturing. In the mylonitic granites, a fine-grained matrix composed of quartz, biotite, sericite, and chlorite wraps rotated porphyroclasts of quartz, plagioclase, and K-feldspar. The ultramylonitic granites display a few strongly fractured porphyroclasts of K-feldspar in a fine-grained matrix of quartz, muscovite, and chlorite with minor calcite and biotite.

Basic and acidic volcanic rocks also were recognized in this profile. Acidic rocks consist of a 1 m thick belt of porphyritic rocks with 30% euhedral quartz, plagioclase ($An_{10–15}$), and K-feldspar phenocrysts in a groundmass of microcrystalline quartz, alkaline feldspar, and fine micas. Quartz shows embayment, whereas plagioclase forms agglomerates. Its microscopic characteristics and QAP diagram classification correspond with a rhyolite.

Basic vulcanites appear as a 10 m thick, 90 m long body with notable coarse fenocrysts of plagioclase. Kilmurray (1968b) first described these rocks as diabases. The groundmass displays a pilotaxitic texture with laths of plagioclase and elongated crystals of tremolite, epidote, and quartz. The plagioclase ($An_{20–23}$) shows alteration to epidote and sericite. Oscillatory zoning and lamellar twinning are common. On the basis of these characteristics, the rocks are classified as andesites.

2.1.2. Cerro del Corral

Cerro del Corral is located 1000 m east of Pan de Azucar, and together they constitute the core of a large overturned anticline. Ductile shear zones and belts of mylonites and phyllonites on the eastern side of Cerro del Corral are related to overthrusting on the Paleozoic sequences. Protoclastic, protomylonitic, and mylonitic granites appear on the western flank of the Cerro del Corral (Fig. 2b). They are coarse- to medium-sized grains with fractured quartz, K-feldspar, and twinned plagioclase ($An_{8–10}$). Secondary quartz, biotite, and muscovite appear in veinlets or disseminated crystals. On a QAP diagram, these rocks plot in the synogranite and monzogranite fields.

Volcanic rocks display porphyritic, protomylonitic, and mylonitic textures. Porphyritic varieties are composed of 20% quartz, alkali feldspar, and plagioclase phenocrysts. Quartz appears as subhedral phenocrysts with embayment and shadowy extinction. The alkali feldspars are euhedral and exhibit simple twinning and flame-like pertites. The scarce plagioclase phenocrysts ($An_{10–12}$) have diffuse lamellar twinning. The matrix consists of muscovite, biotite, calcite, subhedral quartz, and plagioclase (An_{10}). They are petrographically classified as rhyolites.

Micaceous-rich, coarse bands of quartz and alkali feldspar compose the mylonitized rhyolites. The original igneous quartz and alkali feldspar represent porphyroclasts or augens surrounded by a deformed matrix.

2.1.3. Cerro San Mario

In Cerro San Mario, an east–west, elongated, granitic body (600 m long, 150 m wide) is overthrust on conglomerates of the Curamalal Group. The San Mario granite is a medium- to coarse-grained biotite monzogranite with protoclastic to protomylonitic textures (Fig. 2c). The mineralogy consists of quartz, K-feldspar, plagioclase, and biotite. Plagioclase ranges from $An_{15–33}$ in syenogranites to $An_{26–40}$ in monzogranites. Large alkali feldspar is usually perthitic and shows shadowy, crosshatched twinning.

Several foliated belts cut the granite N–S (353°/66°SW). Minor aplite and pegmatite dikes cross-cut the granites. Delpino and Dimieri (1992) recognized two deformational events. The first is evidenced by a regional NNW schistosity, and NE shear planes represent the second.

2.2. Cochenleufú suite

2.2.1. Agua Blanca

The Agua Blanca granite occurs 10 km north of Cerro Pan de Azúcar. It is a porphyritic to aplitic granite, composed of microcline, anorthoclase, quartz, and plagioclase. Quartz appears as isolated phenocrysts, whereas plagioclase ($An_{0–5}$) is subhedral to euhedral. Biotite with strong pleocroism and muscovite are scarce. Fluorite is present as disseminated crystals or veinlets in the microcline (Grecco, 1990). Most samples from the Agua Blanca granite plot on the monzogranite field in a QAP diagram (Fig. 2d). Dimieri et al. (1990) described kink bands, deformational twinning, and flexures in microcline and biotite crystals, suggesting ductile deformation during the solid-state stage (Simpson, 1985; Paterson et al., 1989).

2.2.2. La Ermita

La Ermita is located 10 km NNW of Agua Blanca. It forms a N–S, 500 m long hill with no relationships to the Paleozoic cover. These rocks display fluidal and microporphyritic textures with quartz and K-feldspar phenocrysts. Quartz is anhedral and presents undulose extinction and parallel deformational bands. The groundmass is completely recrystallized to fine-grained quartz. Fluorite and iron oxides appear as disseminated crystals. These rocks are classified as rhyolites.

2.2.3. Cerro Colorado

Cerro Colorado is located 20 km W of Cerro San Mario. The predominant lithology is a medium to coarse granite (Fig. 2d). Microcline, quartz, and plagioclase are the most abundant minerals; biotite, muscovite, fluorite, zircon, apatite, and magnetite are accessory minerals. Quartz appears in small- to medium-size clusters between microcline or as large phenocrysts. Microcline appears as large (3–5 cm) euhedral to subhedral crystals. Plagioclase ($An_{6–10}$) is euhedral with crystals up to 10 mm long, often twinned according to albite and albite-carlsbad. Micaceous minerals are pleochroic biotite and kink-banded muscovite flakes. Fluorite appears as disseminated crystals in K-feldspar, irregular veinlets, and small lenses.

The western side of Cerro Colorado contains a foliation marked by the orientation of K-feldspar megacrysts (3–5 cm long) and mica flakes. The K-feldspar megacrysts are aligned in two trends: L1 (55°–65°/N300°–120°) and L2 (55°–65°/N20°–200°). Biotites display a 289°/44°SW to 340°/35°SW foliation. Biotite cumulates also follow this foliation. Orientations of feldspar and micas form an angle of 20°–40° and display a S–C foliation. This fabric was developed during a submagmatic stage (Miller and Paterson, 1994; Tribe and D'Lemos, 1996). Dimieri et al. (1990) described similar features in the Agua Blanca granite.

3. Geochemistry systematics

Major, trace, and rare earth elements (REE) geochemical data for both suites appear in Tables 1 and 2. X-ray fluorescence was used to determine major, minor, and trace elements: SiO_2, TiO_2, Al_2O_3, FeO, MnO, MgO, CaO, Na_2O, K_2O, P_2O_5, Ba, Cl, Co, Cr, Cu, Ga, Nb, Pb, Rb, Sr, Th, U, V, Y, Zn, and Zr. International geostandards, including AC-E, MA-N, GS-N, GA, and GH granitoids, were used for instrumental calibration. The analyses were carried out at University of Barcelona. Instrumental neutron activation analyses (INAA) were carried out on 31 selected samples to determine the REE, Ta, Hf, Sc, Cs, and Sn at ACTBLABS.

3.1. Meyer suite

3.1.1. Major elements

The granitoids of the Meyer suite are the most mafic of the Sierra de la Ventana igneous rocks, ranging in composition from monzonite to granite (Table 1). Harker diagrams of major elements display decreasing TiO_2, Al_2O_3, Fe_2O_3, MgO (Fig. 3a–d), and CaO and increasing K_2O with increasing fractionation, thus implying a comagmatic origin for these rocks. SiO_2 concentrations are between 57–77 wt% in the Pan de Azucar granite, 67–76 wt% in the Cerro del Corral granite, and 68–76 wt% in San Mario. The granitoids are characterized by high K_2O (Cerro del Corral and Pan de Azucar: 6.29 wt%, San Mario: 5.28 wt%) and fall in the shoshonitic and high-K calc–alkaline fields of Pecerrillo and Taylor's (1976) classification.

The AFM diagram (not shown) indicates a calc–alkaline evolution, with A ranging from 55 to 85 and evolving from the Pan de Azucar andesite to the Cerro del Corral rhyolite. The granitic rocks occupy the transitional terms of this series. All samples are subalkaline.

The ASI index ranges 0.83–2.3 for the Cerro Corral and Pan de Azucar granites and 1.9–1.1 for San Mario; for the Pan de Azucar andesite, it is 1.3, and for the Cerro del Corral rhyolites, it ranges 1.0–3.0. This range plots in the peraluminous field on Shand's (1943) diagram (not shown).

The normative corundum reaches 8.9% in the Cerro del Corral granite, 9.4% in Pan de Azucar, and 7.1% in San Mario, though modal corundum was not recognized. On the basis of their petrographical and geochemical characteristics, the Cerro del Corral, Pan de Azucar, and San Mario granites are interpreted as S-types as suggested by Grecco et al. (1998). The Cerro del Corral rhyolites plot in the peraluminous field of Shand's (1943) diagram and in the banakite and high-K rhyolite field of Pecerrillo and Taylor's (1976) classification.

3.1.2. Trace and REE

Granites of the Meyer suite display significant variations in trace element contents (Table 1). Fractional crystallization is well represented by the K/Rb ratio, which decreases from 401 to 184 in the Pan de Azucar granite, from 261 to 189 in the Cerro del Corral granite, and from 252 to 197 in the San Mario granite. With increasing fractionation, Ba, Sc, Mn, and Zr decrease, and Ga, Ta, Nb, and Y increase (Fig. 3e–h). This indicates fractional crystallization of plagioclase and K-feldspar in the melt, with enrichment of Rb and depletion of Sr in later stages (Grecco et al., 1998).

The total REE reaches 539 ppm in Pan de Azucar, 195 ppm in Cerro del Corral, and 180 ppm in San Mario. Chondrite-normalized spider diagrams of Pan de Azucar (Fig. 4a) indicate strong enrichment of LREE. The La_N/Lu_N between 16 and 100 suggests that garnet remained as a residual phase during the melting of the parental rocks.

The patterns for Cerro del Corral (Fig. 4b) also display important LREE enrichments, though not as high as those of Pan de Azucar. Their La_N/Lu_N relationships vary between 8.6 and 28.0 with small Eu anomalies, reflecting some plagioclase fractionation. San Mario displays patterns similar to those of Cerro del Corral, with La_N/Lu_N relationships varying between 7.6 and 10.2 (Fig. 4c).

The Pan de Azucar andesite was classified by Winchester and Floyd (1977) as andesite and alkaline basalt. The total REE concentration reaches 83 ppm, with La_N/Lu_N of 5.35 and Eu/Eu* of 0.82 (Fig. 4d).

The Cerro del Corral rhyolite has a high concentration of silica and alkalies, thus classifying it as a high-K subalkaline (Leat et al., 1986). The total REE concentration reaches 164 ppm. Chondrite-normalized diagrams (Fig. 4b) display severe negative Eu anomalies (Eu/Eu*: 0.097–0.42), which indicate that plagioclase was strongly fractionated.

3.2. Cochenleufú suite

3.2.1. Major elements

The Agua Blanca and Cerro Colorado granites present very restricted chemical compositions (Table 2) with $SiO_2 = 73–77$ wt%, $Al_2O_3 = 11–17$ wt%, and $K_2O = 3.84–6.36$ wt%. Fractional crystallization is not evident from the Harker diagrams (Fig. 3a–d). The Agua Blanca and Cerro Colorado granites are peraluminous

Table 1
Chemical analyses of the Meyer suite (major elements in wt%, trace, and REE in ppm)

Sample	CR0590	CR0190	PA 0991	PA 0491	PA0891	PA2191	PA2291	PA1891	PA0291	PA0791	PA1691	SM 0292	SM 0492	SMO2	SM 0192	SM 0392	PA 1991	CR0791	CR0690	CR0391
Locality	Corral Granite	Corral Granite	Pan Azucar	Pan Azucar	Pan Azucar	Pan Azucar	Pan Azucar	Pan Azucar	Pan Azucar	Pan Azucar	Pan Azucar	San Mario	San Mario	San Mario	San Mario	San Mario	Azucar Ande-site.	Corral Rhyolite	Corral Rhyolite	Corral Rhyolite
SiO_2	67.96	68.44	72.93	72.54	74.81	61.59	60.75	57.01	67.53	69.93	65.05	68.36	76.09	72.89	70.67	68.21	60.71	76.49	74.58	73.05
TiO_2	0.68	0.54	0.56	0.52	0.35	0.55	0.63	0.91	0.43	0.73	0.80	0.33	0.21	0.27	0.30	0.52	0.78	0.09	0.07	0.07
Al_2O_3	16.47	15.37	15.79	16.26	13.98	15.85	15.79	17.44	15.91	15.81	16.29	15.51	14.75	14.78	15.16	16.35	16.41	13.36	13.01	17.15
FeO	4.24	2.80	1.99	1.60	1.35	4.28	4.30	6.45	4.42	2.66	3.56	2.34	1.08	1.19	1.94	3.05	5.81	0.78	1.11	1.46
MnO	0.05	0.04	0.02	0.02	0.03	0.14	0.11	0.24	0.15	0.03	0.04	0.06	0.01	0.03	0.06	0.05	0.25	0.07	0.02	0.01
MgO	1.27	0.92	0.76	0.63	0.78	2.05	2.10	1.51	1.43	1.18	1.32	0.49	0.38	0.34	0.76	1.35	1.46	0.13	0.06	0.44
CaO	0.67	0.46	0.13	0.32	1.73	1.82	1.68	1.79	2.05	0.56	2.32	1.52	0.24	0.89	0.87	3.15	2.88	1.23	0.24	0.00
Na_2O	0.87	2.50	0.77	0.14	0.57	4.59	6.99	3.89	0.26	1.75	1.57	3.24	1.02	2.23	2.40	0.31	0.10	0.34	3.60	0.24
K_2O	4.91	5.32	5.95	5.59	3.99	4.35	4.04	6.29	5.13	5.50	5.12	5.28	5.21	5.11	5.10	4.53	6.05	4.89	5.10	4.91
P_2O_5	0.24	0.17	0.17	0.09	0.09	0.16	0.18	0.14	0.05	0.12	0.20	0.13	0.06	0.05	0.13	0.06	0.10	0.01	0.02	0.02
LOI	1.93	2.93	1.37	2.00	2.34	3.12	2.06	3.45	1.98	1.32	3.00	2.32	1.82	1.57	1.18	1.90	4.74	1.89	1.19	2.05
Cr	8	10	5	5	17	27					23	18	13	21	14	48	410	6	2	12
Co	44	57	55	72	73	46					64	67	86	104	53	87	34	83	110	47
Sc	11	4	3	5	2	10					6	4	3	5	4		25	4	4	3
V	45	41	23	30	24	65	65	121	38	47	68	27	8	15	20	63	119	1	2	8
Rb	170	208	192	179	107	109	83	284	167	197	166	205	177	220	174	149	266	1.00	1.00	1.00
Cs	2.00	2.00	22.00	1.00	2.00	3.00					3.00	3.00	1.00	3.00	4.00		9.00	274	285	555
Ba	1441	1073	794	1416	460	650	652	1169	765	753	1064	1177	752	579	1201	427	1026	102	56	20
Sr	105	143	170	238	161	410	356	38	82	191	191	122	99	98	223	216	60	20	21	16
Ga	18	21	16	16	14	19	20	18	15	16	21	17	15	17	17	19	15	3.20	4.00	2.00
Ta	0.50	1.00	4.98	5.50	1.00	2.00					4.00	4.98	5.00	3.04	0.50	5.53	8.86	25.3	40.9	24.6
Nb	22.9	17.3	9.4	13.8	11.0	14.2	15.3	18.8	18.8	1.4	15.6	21.7	23.7	25.6	17.9	17.1	18.0	7.00	8.00	5.00
Hf	10.00	8.00	9.00	12.00	5.00	6.00					10.00	5.00	5.00	7.00	7.00		6.00	153	148	97
Zr	291	200	265	386	243	180	171	113	166	420	254	181	137	145	232	177	109	37	80	23
Y	27	9	19	22	11	10	11	21	36	21	11	22	24	31	18	11	18	26.34	41.48	18.55
Th	8.20	21.12	95.19	61.09	61.58	5.80	7.88	3.84	11.07	142.17	24.42	13.37	18.01	25.19	10.42	17.67	4.23	1.30	8.19	3.75
U	0.20	0.40	1.40	1.10	1.93	0.40					1.2	2.30	1.11	2.60	0.40		1.10	38.00	22.00	19.00
La	49.00	34.00	150.00	120.00	94.00	30.00					80.00	37.00	38.00	51.00	44.00		21.00	75.00	53.00	35.00
Ce	88.00	77.00	240.00	210.00	170.00	54.00					150.00	65.00	67.00	81.00	81.00		38.00	38.00	34.00	14.00
Nd	45.00	30.00	130.00	96.00	81.00	22.00					61.00	22.00	32.00	35.00	34.00		15.00	6.40	8.20	2.50
Sm	7.00	4.60	16.00	11.00	10.00	4.20					9.60	3.70	4.50	6.00	3.90		3.80	0.20	0.20	0.40
Eu	1.40	0.60	0.90	1.30	1.10	1.40					1.50	0.80	0.90	1.00	1.00		1.10	1.20	1.90	0.60
Tb	1.00	0.50	0.41	0.50	0.50	0.40					0.48	0.50	0.50	0.40	0.50		0.80	5.05	9.06	3.07
Yb	3.83	1.20	1.64	3.51	0.92	1.54					1.21	3.22	4.01	5.43	2.66		3.21	0.67	1.27	0.45
Lu	0.61	0.13	0.20	0.54	0.10	0.20					0.16	0.49	0.53	0.70	0.46		0.42	6.54	6.51	19.71
Cl	b.d.	40.47	14.20	14.26	13.06	26.47	27.08	7.12	11.05	33.57	18.47	17.07	58.96	97.90	32.39	26.96	17.68			

Table 2
Chemical analyses of the Cochenleufú suite (major elements in wt%, trace, and REE in ppm)

Sample	AB 02	AB 09	AB 15	AB 14	AB 03	AB 17 g	AB 1884	AB 2284	AB 17r	AB 1722	AB 1384	AB 0884	AB 0384	CC 02	CC 04	CC 05	CC 08
Locality	Agua Blanca	Agua Blanca	Agua Blanca	Agua Blanca	Agua Blanca	Agua Blanca	Agua Blanca	Agua Blanca	Agua Blanca	Agua Blanca	Agua Blanca	Agua Blanca	Agua Blanca	Cerro Colorado	Cerro Colorado	Cerro Colorado	Cerro Colorado
SiO_2	75.89	74.33	75.31	73.26	74.35	75.33	76.32	74.37	74.18	76.37	73.03	77.01	76.23	77.18	77.36	75.49	76.09
TiO_2	0.04	0.05	0.03	0.12	0.02	0.05	0.02	0.02	0.05	0.02	0.05	0.02	0.06	0.08	0.11	0.10	0.11
Al_2O_3	12.85	13.95	13.29	14.30	13.29	13.89	13.36	12.94	13.35	13.77	13.64	13.84	13.84	11.95	11.63	12.99	12.34
FeO	1.35	1.09	1.63	1.01	1.29	1.75	0.36	0.91	1.25	0.77	1.20	0.49	0.63	0.85	0.93	1.04	1.22
MnO	0.23	0.19	0.10	0.08	0.09	0.49	0.33	0.10	0.49	0.09	0.11	0.08	0.04	0.01	0.01	0.01	0.03
MgO	0.15	0.04	0.42	0.03	0.06	0.19	0.02	0.01	0.11	0.01	0.12	0.06	0.09	0.10	0.10	0.10	0.10
CaO	0.70	0.10	0.21	0.70	0.90	0.16	0.29	0.37	0.13	0.39	0.15	0.11	0.50	0.10	0.17	0.26	0.28
Na_2O	3.20	4.43	4.34	4.22	3.79	3.68	2.37	6.00	3.68	0.59	5.46	2.80	2.75	3.27	3.17	3.65	3.48
K_2O	4.64	4.26	4.20	4.14	4.45	4.26	5.33	4.80	4.26	4.82	5.10	4.76	4.79	5.73	4.68	5.25	4.88
P_2O_5	0.03	0.03	0.01	0.02	0.01	0.01	0.00	0.00	0.01	0.00	0.00	0.01	0.01	0.01	0.02	0.01	0.02
LOI	0.87	0.50	0.52	0.40	0.60	0.21	1.54	0.25	0.50	0.64	0.45	0.63	0.79	0.62	0.27	0.32	0.32
Cr							350			15	47	360	310				
Co							4			97	78	3	4				
Sc									3	10	17	6	5				
V									4	1	9	4	1				
Rb					440	490	524	783		773	558	533	455				
Cs							9.00			23.00	3.00	6.00	5.00				
Ba							110	7		240	47	170	30				
Sr					8	5	20	1	27	2	8	8	5				
Ga							24	26	15	28	22	24	20				
Ta									5.00	7.93	4.00	4.00	5.00				
Nb					51.0	46.0	52.5	57.3	51.0	58.5	52.3	52.9	72.9				
Hf							3.00			16.00	14.00	6.00	6.00				
Zr					74	152	30	133	64	132	85	67	75				
Y					64	150	63	173	101	184	87	169	93				
Th							29.46	42.95	15.00	45.83	52.92	24.85	62.48				
U							3.14		4.50	4.10	4.00	2.00	3.50				
La									18.00	14.00	110.00	13.00	16.00				
Ce									49.00	54.00	170.00	33.00	37.00				
Nd									17.00	16.00	71.00	25.00	23.00				
Sm									6.70	9.40	13.00	7.70	7.60				
Eu									0.20	0.20	3.10	0.30	0.20				
Tb									2.10	2.60	0.20	2.20	1.80				
Yb									10.90	29.70	3.59	18.70	11.60				
Lu									1.32	3.90	0.53	2.73	1.66				
Cl							100.70	30.68	31.40	35.01	33.59	68.00	39.58				

Sample	CC 20	CC 23	CC 24	CC 26	CC 1683	CC 1983	CC 2283	CC 3183	CC 0183	CC 02b	CC 03
Locality	Cerro Colorado	Cerro Colorado	Cerro Colorado	Cerro Colorado	Cerro Colorado	Cerro Colorado	Cerro Colorado	Cerro Colorado	Cerro Colorado	Cerro Colorado	Cerro Colorado
SiO_2	76.45	74.01	74.75	76.91	75.98	76.59	77.40	77.50	77.80	74.27	76.18
TiO_2	0.06	0.06	0.08	0.04	0.09	0.07	0.06	0.06	0.10	0.08	0.05
Al_2O_3	12.29	13.32	13.65	12.75	13.05	13.05	13.56	12.86	13.37	13.07	12.52
FeO	0.86	1.40	1.22	0.43	1.16	0.77	0.89	0.99	1.13	1.17	1.22

(continued on next page)

Table 2 (*continued*)

Sample	CC 20	CC 23	CC 24	CC 26	CC 1683	CC 1983	CC 2283	CC 3183	CC 0183	CC 02b	CC 03
Locality	Cerro Colorado	Cerro Colorado	Cerro Colorado	Cerro Colorado	Cerro Colorado	Cerro Colorado	Cerro Colorado	Cerro Colorado	Cerro Colorado	Cerro Colorado	Cerro Colorado
MnO	0.01	0.01	0.01	0.01	0.03	0.01	0.01	0.02	0.01	0.01	0.01
MgO	0.10	0.06	0.09	0.20	0.09	0.07	0.05	0.03	0.22	0.12	0.01
CaO	0.10	0.87	0.50	0.54	0.38	0.59	0.40	0.32	0.10	0.10	0.46
Na_2O	4.00	3.49	3.83	3.97	3.22	3.58	1.71	2.40	1.50	2.90	4.07
K_2O	4.83	4.88	4.91	4.33	5.12	4.96	5.17	5.12	5.30	6.36	3.84
P_2O_5	0.02	0.02	0.02	0.02	0.01	0.01	0.00	0.00	0.01	0.02	0.01
LOI	0.10	0.51	0.21	0.37	0.68	0.17	0.64	0.53	0.32	0.32	0.19
Cr					2	3	6	5	4		
Co					4	3	3	1	4		
Sc					4	4	4	3	5		
V					10	5	6	2	2		
Rb					394	423	467	262	352		
Cs					17.00	17.00	9.00	5.00	9.00		
Ba					67	51	45	140	126		
Sr					8	7	9	16	7		
Ga					23	24	24	19	20		
Ta					3.00	5.00	4.00	3.00	2.00		
Nb					40.9	46.8	46.2	39.1	37.1	29.0	
Hf					11.00	10.00	7.00	4.00	6.00		
Zr					140	121	79	34	104	107	
Y					96	129	98	77	53	79	
Th					66.17	64.18	46.37	53.75	33.56		
U					4.06	9.66	3.50	1.90	3.30		
La					29.00	26.00	19.00	15.00	39.00		
Ce					77.00	79.00	53.00	43.00	81.00		
Nd					34.00	30.00	22.00	23.00	39.00		
Sm					12.00	14.00	9.30	9.80	9.00		
Eu					0.30	0.40	0.20	0.20	0.40		
Tb					3.20	3.40	2.70	2.20	1.90		
Yb					13.90	18.20	12.90	10.30	6.13		
Lu					1.67	2.26	1.67	1.26	0.88		
Cl					32.87	33.28	32.75	30.27	35.15		

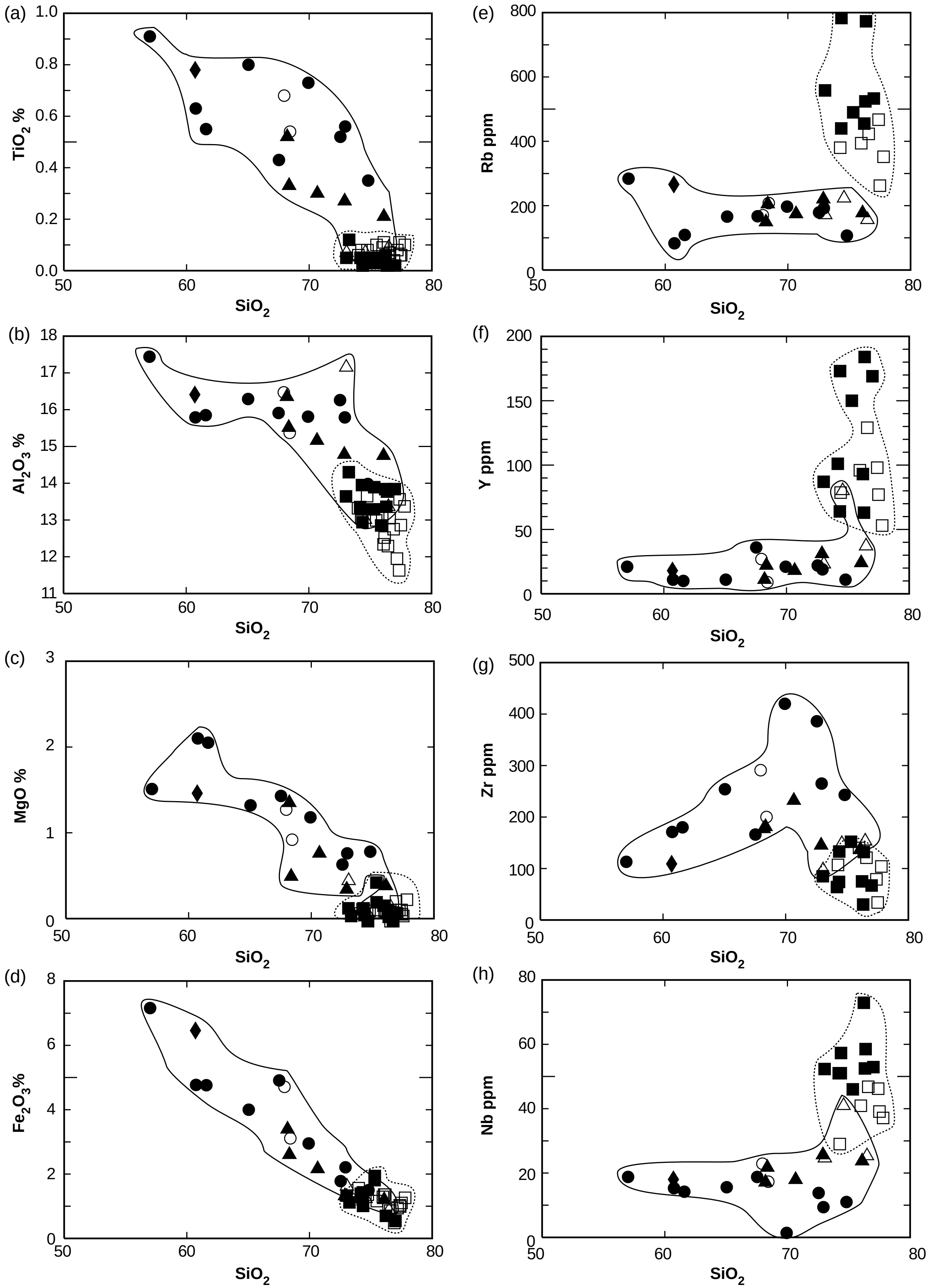

Fig. 3. Harker diagrams for the Meyer and Cochenleufú suites. Pan de Azucar granite ●, Cerro del Corral granite ○, San Mario granite ▲, Cerro del Corral rhyolite △, Pan de Azucar andesite ♦, Agua Blanca granite ■, and Cerro Colorado granite □.

and subalkaline with 6.8 and 4.4 wt% corundum normative, respectively.

3.2.2. Trace and REE

The Agua Blanca and Cerro Colorado granites present restricted trace element concentrations, with Rb, Y, Nb, and Ga higher than those of the Meyer suite, whereas the Sr, Zr, and Ba concentrations are lower (Fig. 3e–h). Logarithmic plots of Rb–Sr and Ba–Rb indicate restricted fractional crystallization of plagioclase and K-feldspar (see Grecco et al., 1998). Total REE concentrations are between 104 and 177 ppm in Cerro Colorado and between 98 and 370 ppm in Agua Blanca. The chondrite-normalized diagram for the Cochenleufú suite indicates enrichments of 60–150 times in Cerro Colorado and 50–400 times in Agua Blanca (Fig. 4e and f). Both bodies have strong negative Eu anomalies with Eu/Eu* = 0.049–0.094 in Agua Blanca and 0.051–0.127 in Cerro Colorado. These strong negative Eu anomalies indicate that plagioclase was severely fractionated from the original magma.

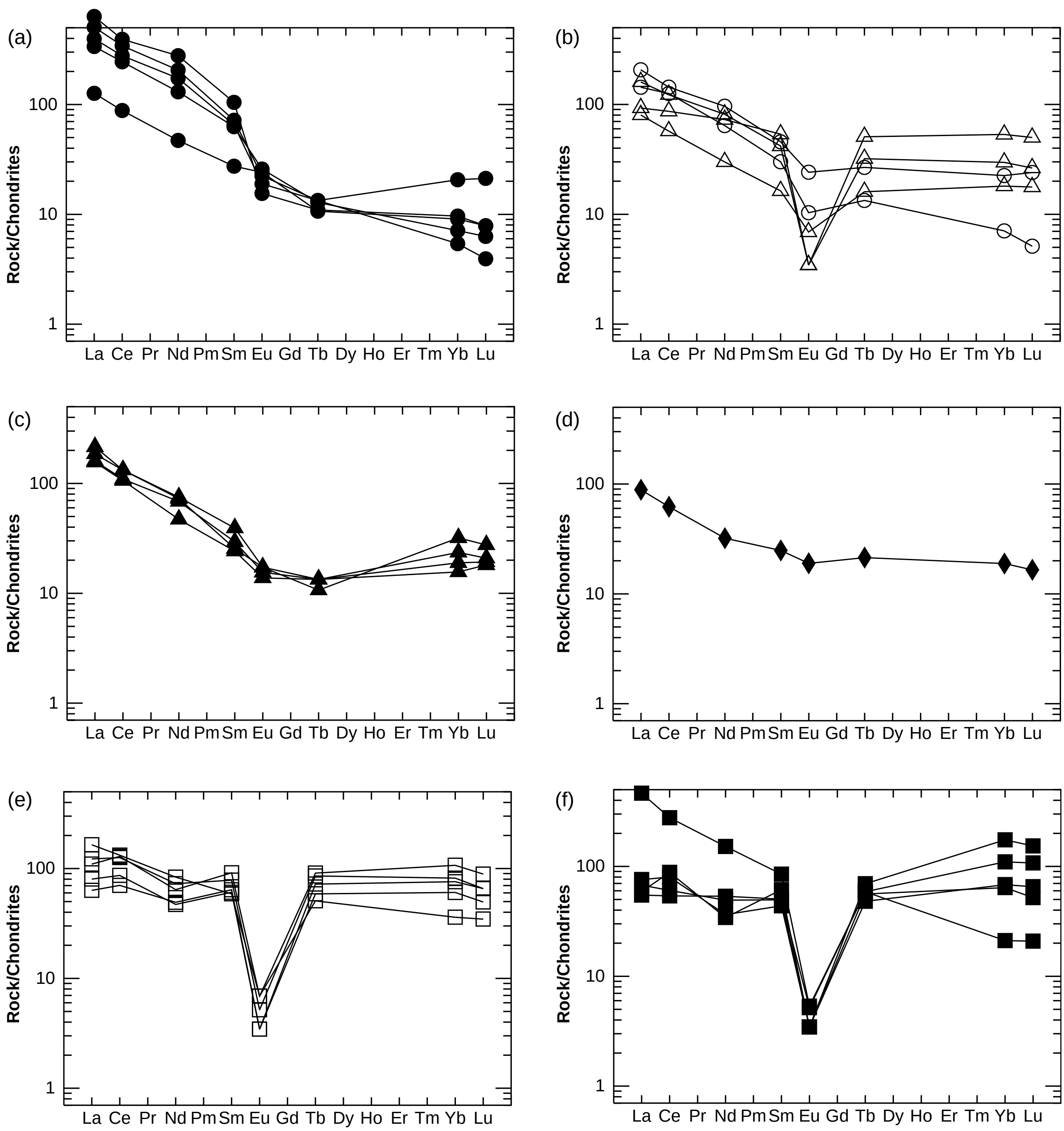

Fig. 4. Chondrite-normalized spider diagrams for (a) Pan de Azucar granite, (b) Cerro del Corral granite and rhyolites, (c) San Mario granite, (d) Pan de Azucar andesite, (e) Cerro del Colorado granite, and (f) Agua Blanca granite. Symbols as in Fig. 3.

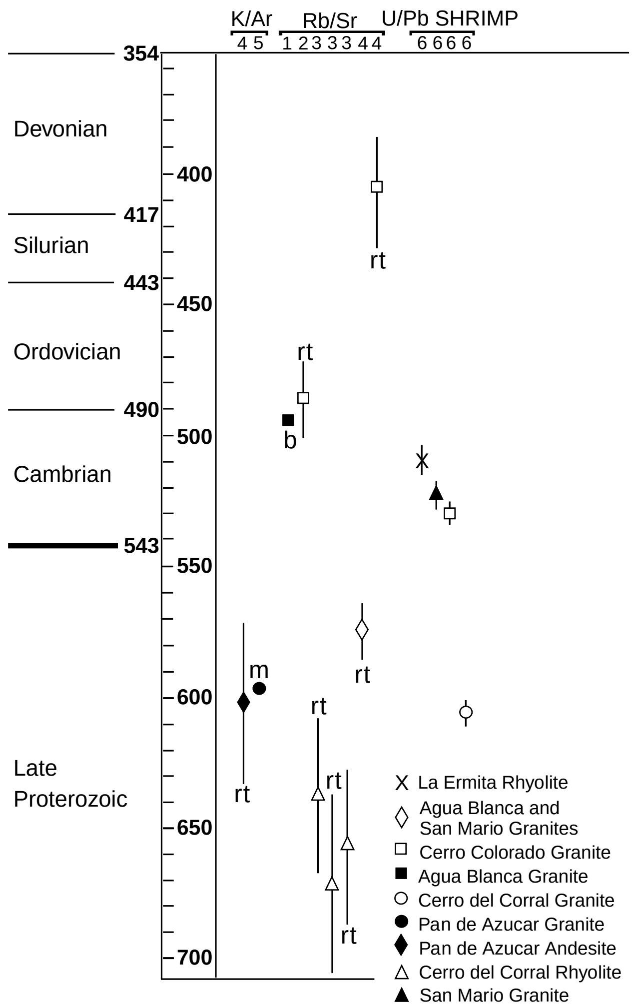

Fig. 5. Radiometric ages obtained from Sierra de la Ventana. (1) Borrello and Venier (1967); (2) Varela et al. (1990); (3) Varela and Cingolani (1975); (4) Cingolani and Varela (1973); (5) Cazeneuve (1967); and (6) Rapela et al. (2003). rt: whole rock, b: biotite, and m: muscovite.

4. Previous geochronological studies

Borrello and Venier (1967), Cazeneuve (1967), Cingolani and Varela (1973), and Varela and Cingolani (1975) obtained radiometric ages for the granitic and volcanic rocks of Sierra de la Ventana using K/Ar and Rb/Sr methods. Rapela et al. (2003), using the U–Pb SHRIMP method, established a clear distinction between Neoproterozoic and Lower Paleozoic ages (Fig. 5).

Late Proterozoic ages were obtained for the Cerro del Corral rhyolite (671 ± 35,655 ± 30,638 ± 30 Ma), Cerro del Corral granite (612.3 ± 5.3, 607 ± 5.2 Ma), Pan de Azucar andesite (603 ± 30 Ma), and Pan de Azucar granite (598 Ma).

Cingolani and Varela (1973) also constructed a Rb/Sr isochron using samples from both the San Mario and Agua Blanca granites to obtain an age of 574 ± 10 Ma. Lower Paleozoic ages were obtained for the Cerro del Colorado granite (487 ± 15, 407 ± 21, 529.6 ± 3.3, 531.1 ± 4.1 Ma), Agua Blanca granite (492 Ma), San Mario granite (524.3 ± 5.3, 526.5 ± 5.5 Ma), and La Ermita rhyolite (509 ± 5.3 Ma).

The age population indicates two magmatic cycles at 700–560 and 530–470 Ma, which are concordant with the field-, petrographical-, and geochemical-based separation into two suites. Discrepancies arise when the younger age of the San Mario granite is compared with other members of the Meyer suite (Rapela et al., 2003). On the basis of the strong geochemical, petrographical, and deformational similarities among the San Mario granite and Pan de Azúcar and Cerro del Corral granites, the San Mario granite is included in the Meyer suite.

Equivalent magmatic cycles have been recognized in South Africa, where they constitute the Cape granite suite (Scheepers, 1995; Scheepers and Poujol, 2002).

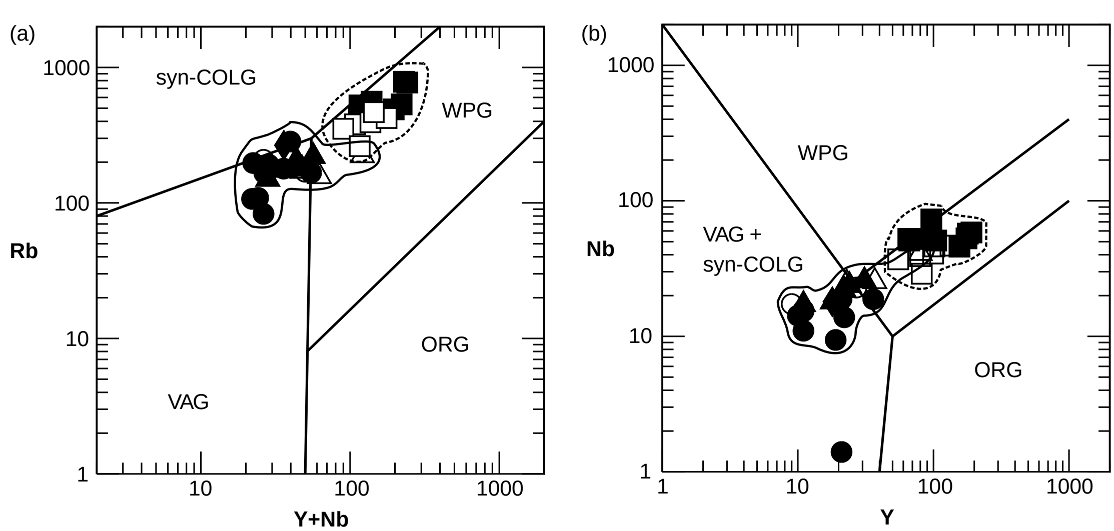

Fig. 6. (a) Rb versus Y + Nb diagram (Pearce et al., 1984) and (b) Y versus b diagram for the Meyer and Cochenleufú suites. Symbols as in Fig. 3.

5. Tectonic discrimination

5.1. Meyer suite

Pearce et al. (1984) subdivided the granitoids, according to their tectonic setting, into intrusion in ocean ridge, volcanic arc, within plate, orogenic, and syncollisional granites. In the Y + Nb versus Rb diagram (Fig. 6a), samples plot dominantly in the volcanic arc field, whereas in the Y versus Nb diagram, they plot in both the volcanic arc and syncollisional fields (Fig. 6b).

Whalen et al. (1987) discriminated between A-type granites and most orogenic granitoids (M-,I-, and S-types) using the Ga/Al relationships and Y, Nb, and Zr concentrations. In Whalen et al.'s (1987) discrimination diagrams, the Meyer suite granites plot in the S- and I-type granite fields (Fig. 7). These results indicate that the Meyer suite consists of S-type granites, as defined by Chappell and White (1974). Grecco et al. (1998) reported the calc–alkaline character of these rocks, as well as their S-type signature. According to Rapela et al. (2003), the San Mario granite is a differentiated I-type granite and not consanguineous with the Agua Blanca granite.

Harris et al. (1986) recognized four groups of granitic rocks in the Himalayan, Alpine, and Hercynian belts: (1) precollisional, calc–alkaline, dioritic to granodioritic plutons associated with volcanic arcs; (2) syncollisional, peraluminous leucogranites; (3) late- or postcollisional, calc-alkaline, biotite-hornblende tonalite to granodioritic plutons; and (4) postcollisional alkaline rocks. In the triangular diagram Rb/30-Hf–Ta*3 (Fig. 8a), samples plot in the precollisional (volcanic arc) and the late- or postcollisional fields, though a few appear in the within-plate field. In the SiO_2 wt% versus Rb/Zr diagram (not shown), most samples plot in the VAG field. In the Y–Nb–Ce and Y–Nb–3*Ga diagrams of Eby (1992), most samples plot (Fig. 9a and b) in the A_1-type granite field.

Rocks with similar geochemical and petrologic characteristics emplaced during a subduction-collision event have been recognized in the Karakoram Axial batholith of northern Pakistan (Baltoro plutonic unit, Hunza leucogranite; Crawford and Windley, 1990), the Pan-African belt of the Arabian shield (Jackson et al., 1984), the Homrit Waggat complex of Egypt (Hassanen, 1997), and the Qinling belt of China (Mattauer et al., 1985).

Through plotting in TiO_2–MnO*10-P_2O_5*10, Ti/100-Zr–Y*3, and Th/Yb–Ta/Yb discriminant diagrams (Pearce and Cann, 1973; Pearce, 1982; Mullen, 1983), the Pan de Azucar andesite is classified as a calc–alkaline basalt that erupted at an active continental margin (not shown).

5.2. Cochenleufú suite

Samples from the Cochenleufú suite plot in the within-plate granite field (Fig. 6) of Pearce et al.'s (1984)

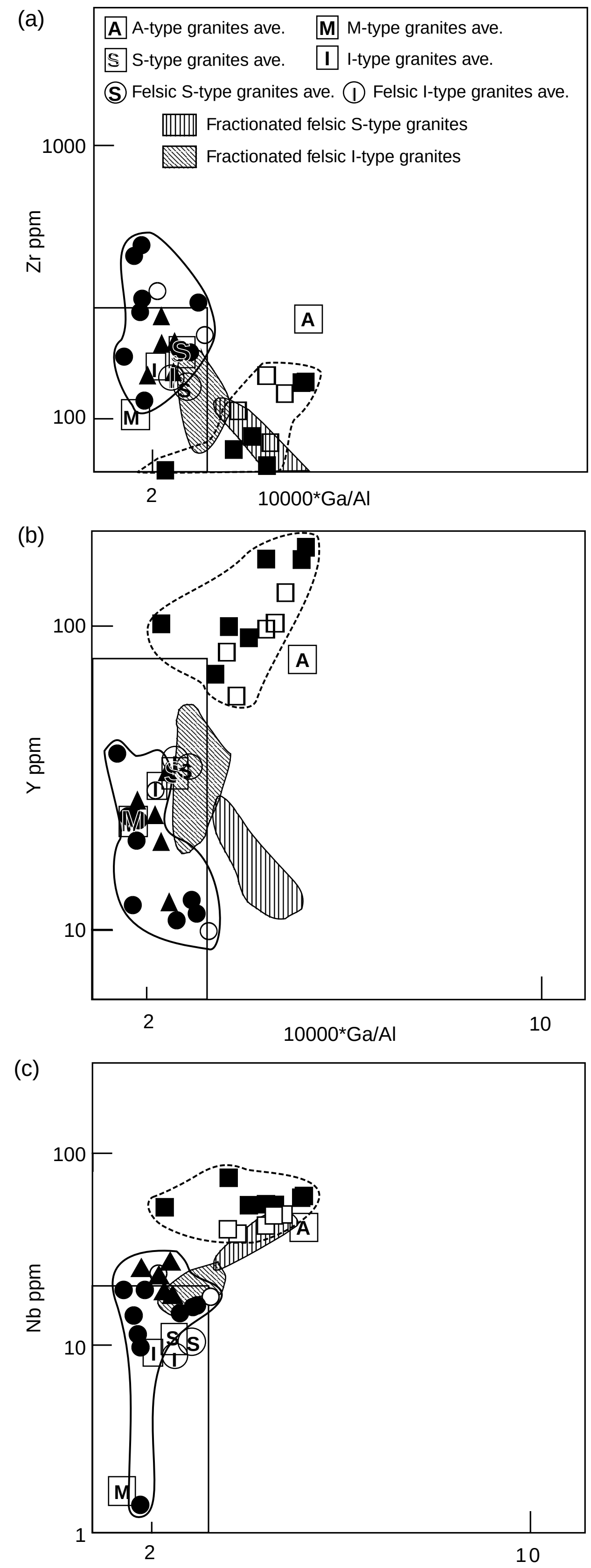

Fig. 7. (a) Zr, (b) Nb, and (c) Y versus 10,000Ga/Al diagrams (Whalen et al., 1987) for the Meyer and Cochenleufú suites. Symbols as in Fig. 3.

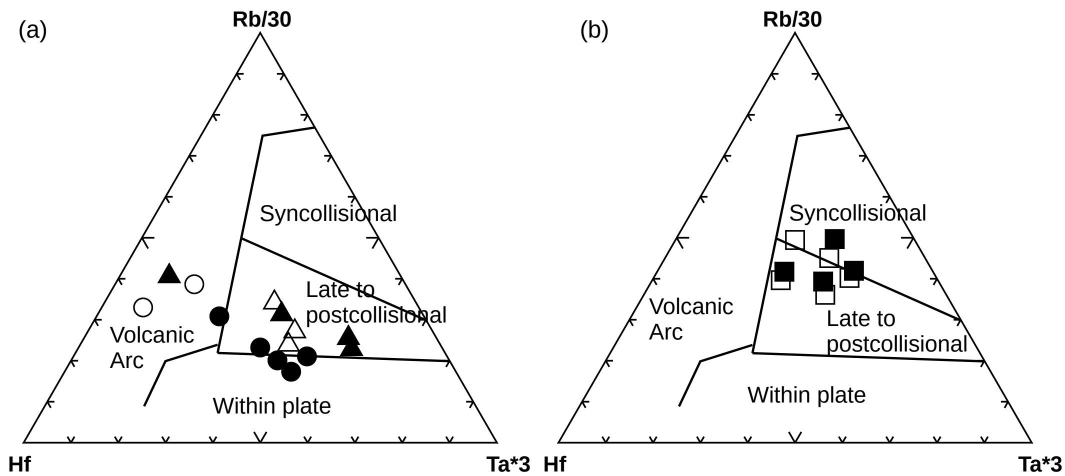

Fig. 8. Rb/30–Hf–Ta*3 diagrams (Harris et al., 1986) for the (a) Meyer and (b) Cochenleufú suites. Symbols as in Fig. 3.

diagrams. They also fall in the A-type granite field in trace elements versus 10,000 Ga/Al discrimination diagrams (Fig. 7). This result is in agreement with Grecco's (1990) conclusion, based on major elements, as well as with Rapela et al.'s (2003) interpretation. These rocks also share some A-type granite characteristics, namely, high SiO_2 and Na_2O+K_2O, low CaO, and high Ga/Al, Zr, Nb, Ga, Y, and Ce.

In the Rb/30-Hf–Ta*3 diagram (Harris et al., 1986), the samples plot in the syn- to postcollisional fields (Fig. 8b); in the SiO_2 wt% versus Rb/Zr diagram (not shown), they are classified in the syncollisional field.

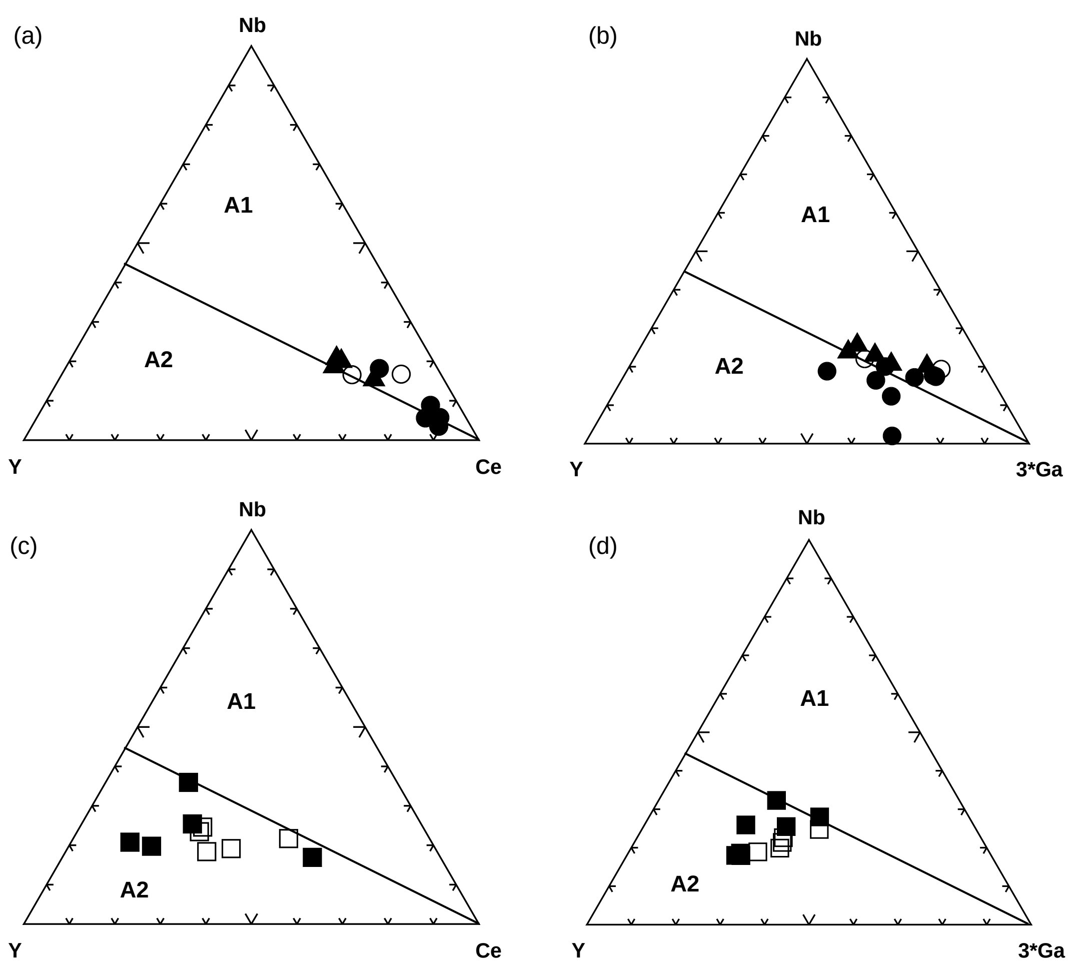

Fig. 9. (a) Y–Nb–Ce diagram (Eby, 1992) and (b) Y–Nb–3*Ga diagram for the Meyer and Cochenleufú suites. Symbols as in Fig. 3.

Finally, in Eby's (1992) Y–Nb–Ce and Y–Nb–3*Ga diagrams, most of the samples plot in the continental–continental collisional to postcollisional field (Fig. 9a and b). This result agrees with Rapela et al. (2003). Examples include the Gabo and Mumbulla suites in the Lachland fold belt, Australia (Collins et al., 1982), and the Topsails complex of Newfoundland (Whalen et al., 1987).

6. Discussion

In Sierra de la Ventana, the deficiency of igneous rock outcrops, as well as the lack of field relationships with host rocks, makes it difficult to establish its tectonic setting. However, the correlation with the African granitic suites (Grecco, 1990) enables us to clarify the evolution of accretional events in Sierra de la Ventana (Table 3). Two igneous suites are differentiated in Sierra de la Ventana. The most basic is the Meyer suite (700–570 Ma), which displays a calc–alkaline evolution related to volcanic arc and postcollisional settings.

In the Saldania belt of South Africa, sedimentary and volcanic rocks deposited in the Boland terrane (Malmesbury Group) attest to ocean floor spreading in response to the breakup of Rodinia and the progressive opening of the proto-Atlantic (Adamastor Ocean) during 780–750 Ma (Rozendaal et al., 1999). Rocks of this age, which represent this extensional event, had not been recognized in Sierra de la Ventana. A reversal of the spreading caused subduction and the closure of the Adamastor Ocean (600–570 Ma). The tholeiitic series (olivine gabbros, gabbros, diorites, and granodiorites) represents this event along an immature magmatic arc (Scheepers, 1995), as does the first phase of intrusion of the Cape granite suite (600–540 Ma). S-type granitic rocks intruded during this phase have late to postorogenic signatures. The presence of a suture zone at the Swartland–Boland terrane boundary supports either oblique collision or strike–slip transpressional tectonics without the development of a collisional orogen. In Sierra de la Ventana, the most basic rocks form the Meyer suite (700–570 Ma), which displays a calc-alkaline evolution. These rocks are related to an immature volcanic arc, but they also show characteristics of a postcollisional setting. In the Cape granite suite, the final phase of intrusion (520–500 Ma) is represented by A-type granitoids (Scheepers, 1995). These anorogenic alkaline granites are related to pressure release in a strike-slip tectonic environment with associated uplift and extension following collision.

The Cochenleufú suite (540–470 Ma) is considered an A-type association and plots in the within-plate, syn- to postcollisional fields in several discrimination diagrams. According to Eby (1992) classification, these rocks belong to the A_2 granitoids, which generally occur as final plutonic events during postorogenic extension in collisional belts (Crawford and Windley, 1990; Bonin, 1990). This magmatic event already has been interpreted as within-plate magmatism and correlated with the Cape granite suite by Grecco and Gregori (1993) and Rapela et al. (2003).

Equivalent postcollisional granites, intruded during an oblique N–S collision of the Kalahari and Congo cratons, have been recognized in the central Damaran orogenic belt, Namibia (Gresse and Scheepers, 1993). They are related to the closure of the Adamastor Ocean.

The Swartland and Tygerberg terranes (Saldania belt), accreted in a transpressive regime to the Boland terrane (600–630 Ma), are potential candidates for the Meyer and Cochenleufú suites' emplacement.

Similar structural styles, magmatism, and tectonic events have been recognized in the Saldania, Ross, and Delamarian orogens, indicating a common history (Rozendaal et al., 1999). The Ross event, responsible for major magmatism in the Transantarctic Mountains, is represented partially by the granitic Harbour intrusive complex (Gunn and Warren, 1962), which was emplaced in a calc–alkaline arc. The Mid-Proterozoic–Late Cambrian history of the Transantarctic Mountains has been interpreted as a cycle of extension,

Table 3
Comparison of tectonic events between Saldania belt and Sierra de la Ventana

Saldania Belt	Sierra de la Ventana
Ocean floor spreading due to break-up of Rodinia and opening of the Adamastor Ocean. Sedimentation and volcanism represented by the Malmesbury group (780–750 Ma)	Not recognized
Subduction and closure of the Adamastor Ocean. Immature magmatic arc. Tholeiitic series and the first phase of Cape granite suite (600–540 Ma) Oblique collision or strike-slip transpressional without a collisional orogen: S-type granitic rocks with late to postorogenic signatures.	Volcanic-arc and postcollisional settings. No collisional orogen recognized Calc–alkaline granites and volcanic rocks of Meyer suite (700–570 Ma)
Island arc or active continental margin subduction–related magmatism Second phase of Cape granite suite (560–520 Ma)	Post-orogenic extension
Uplift and extension after collision during a strike-slip regime Third phase of Cape granite suite (520–500 Ma). Anorogenic alkaline granites	A_2 granitoids of the Cochenleufú suite (540–470 Ma) related to final plutonic events.

Notes: Information about the Saldania Belt after Rozendaal et al. (1999), Scheepers (1995), and Scheepers and Poujol (2002).

continental rifting, transpression, and subduction (Moyes et al., 1993).

Rapela et al. (2003) interpreted the basement complex of the Sierra de la Ventana fold belt as related to Early to Mid-Cambrian continental rifting along the southwestern margin of Gondwana. They correlated the extensional event with similar scenarios in the Cape fold belt, the Atlantic coast of Brazil, the Malvinas microplate, and the Ellsworth Mountains. The A-type granites of the Cochenleufú suite and of the La Ermita rhyolite were formed, according to Rapela et al. (2003), by underplating mafic magma, which melted the lower crust during continental rifting. The absence of mafic rocks related to the Cambrian–Devonian sedimentary sequence precluded correlation with similar rocks in the Ellsworth Mountains, despite magnetic anomalies detected between Sierra de la Ventana and Tandilia. According to Köhn et al. (2002), these anomalies were produced by basaltic rocks below the Paleozoic sequence. However, evidence of such oceanic crust, which must be coetaneous with sedimentation during the Lower Paleozoic, is not present in the Sierra de la Ventana and Claromecó basin (Kostadinoff and Prozzi, 1998).

7. Conclusions

In Sierra de la Ventana, two magmatic suites are differentiated. The older Meyer suite (700–570 Ma) displays a calc–alkaline evolution related to a volcanic arc and postcollisional setting. The younger Cochenleufú suite (540–470 Ma) displays an A-type signature related to the final plutonic events during postorogenic extension in the collisional belts.

The remarkable similarities observed between the suites of Sierra de la Ventana and the Saldania belt enables a positive correlation. In both cases, primitive volcanic arc or collisional orogens are recognized. Moreover, continuous shearing between the Swartland and Tygerberg terranes was a potential trigger for the emplacement of both suites.

Acknowledgements

We thank V. Ramos (UBA), E. Llambías (UNLP), and I. Petrinovic (UNSa) for reviews and comments on an early draft of the manuscript. R. Pankhurst (Keyworth) and C. Rapela (UNLP) are kindly acknowledged for their revision of the final draft of the manuscript. We also thank José L. Fernandez Turiel for helping during X-ray fluorescence analyses. A Marie Curie bursary of the European Community to DAG supported part of this research.

References

Andreis, R.R., 1964. Petrología del Grupo eodevónico de Lolén. Sierras Australes de la Provincia de Buenos Aires. Com. Investig. Científicas. Anal. 5, 79–124. La Plata.

Andreis, R.R., 1989. Cuenca paleozoica de Ventania. Sierras Australes de la provincia de Buenos Aires. In: Chebli, G., Spalletti, L. (Eds.), Cuencas Sedimentarias Argentinas Serie Correlación Geológica. Univ. Nac. Tucumán, pp. 265–298.

Bonin, B., 1990. From orogenic to anorogenic settings: evolution of granitoid suites after a major orogenesis. Geol. J. 25, 261–270.

Borrello, A.V., 1962. Sobre los niveles fosilíferos del Devónico inferior de las Sierras Australes de la Provincia de Buenos Aires. Notas Comisión de Investigaciones Científicas I, 4.

Borrello, A.V., 1964. Los geosinclinales de la Provincia de Buenos Aires, GAEA, Soc. Argentina de Est. Geográficos, Anales, Buenos Aires, XII 1964 pp. 9–19.

Borrello, A., Venier, J., 1967. Nuevas características geológicas del granito Agua Blanca. Dufaur. Prov. de Bs. As. Notas Comisión de Investigaciones Científicas 2, 3–7.

Buggisch, W., 1987. Stratigraphy and very low-grade metamorphism of the Sierras Australes de la Provincia de Buenos Aires (Argentina) and implications in Gondwana correlation. Zentral. Geol. Palaont. Teil I 7/8, 819–837.

Cazeneuve, H., 1967. Edades isotópicas del basamento de la provincia de Buenos Aires. Ameghiniana. Rev. Assoc. Paleont. Arg. 5 (1), 3–10.

Chappell, B.W., White, A.J.R., 1974. Two contrasting granite types. Pacific Geol. 8, 173–174.

Cingolani, C.A., Varela, R., 1973. Examen geocronológico por el método rubidio-estroncio de las rocas ígneas de las Sierras Australes bonaerenses. V Congr. Geol. Arg. Actas 1, 349–371. Buenos Aires.

Cobbold, P.R., Massabie, A.C., Rossello, E.A., 1986. Hercynian wrenching and thrusting in the Sierras Australes Foldbelt, Argentina. Hercynica 2 (2), 135–148.

Collins, W.J., Beams, S.D., White, A.J.R., Chappell, B.W., 1982. Nature and origin of A-type granites with particular reference to Southeastern Australia. Contrib. Mineral. Petrol. 80, 187–200.

Crawford, M.B., Windley, B.F., 1990. Leucogranites of the Himalaya/Karakoram: implications for magmatic evolution within collisional belts and the study of collision-related leucogranite petrogenesis. J. Volcanol. Geoth. Res. 44, 1–19.

Cucchi, R.J., 1966. Petrofábrica del conglomerado de la Formación La Lola, Sierras Australes de la Provincia de Buenos Aires. Rev. Assoc. Geol. Arg. 21, 71–106.

Cuerda, A.J., Cingolani, C.A., Barraquero, H.R., 1975. Estratigrafía del Basamento Precámbrico en la Comarca de los Cerros Pan de Azucar-del Corral. Sierras Australes (Provincia de Buenos Aires). II Congr. Iberoam. Geol. Económ. Actas II, 57–63. Buenos Aires.

Delpino, S., Dimieri, L., 1992. Características de la deformación y cinemática de las rocas del basamento, perfil Las Lomitas, Sierras Australes de Buenos Aires, VIII Reunión de Microtectónica. Actas 1992;, 11–14. Bariloche.

Dimieri, L., Grecco, L., Frisicale, C., 1990. Microestructuras en el Granito Aguas Blancas, Provincia de Buenos Aires, Argentina. Rev. Assoc. Arg. Mineral., Petrol. Sediment. 21 (1-4), 53–60.

Du Toit, A.L., 1937. Our Wandering Continents. Oliver Boyd, Edinburg p. 366.

Eby, G.N., 1992. Chemical subdivision of the A-type granitoids: petrogenetic and tectonic implications. Geology 20, 641–644.

Grecco, L.E., 1990. Geoquímica y Petrología de los intrusivos graníticos Cerros Colorados y Aguas Blancas, Sierras Australes, Provincia de Buenos Aires. Unpublished PhD Thesis, Universidad Nacional del Sur, Bahía Blanca, 159 pp.

Grecco, L.E., Gregori, D.A., 1993. Estudio geoquímico de los intrusivos graníticos Cerros Colorados y Aguas Blancas, Sierras Australes de la provincia de Buenos Aires, Argentina. XII Congr. Geol. Arg. y II Congr. Explor. Hidrocarburos, Actas IV, 81–89. Buenos Aires.

Grecco, L.E., Gregori, D.A., Maiza, P.J., 1984. Relación del contenido de flúor y de OH en las biotitas de las rocas graníticas de la cantera Cerros Colorados, Provincia de Buenos Aires. IX Congr. Geol. Arg., Actas 1984;, 368–375. Buenos Aires.

Grecco, L.E., Gregori, D.A., Ruviños, M.A., 1998. Characteristics of Neoproterozoic magmatism in Sierras Australes. Zentral. Geol. Palaontol. H3-6, 609–619.

Gresse, P.G., Scheepers, R., 1993. Neoproterozoic to Cambrian (Namibian) rocks of South Africa: a geochronological and geotectonic review. J. African Earth Sci. 16 (4), 375–393.

Gunn, G.M., Warren, G., 1962. Geology of Victoria Land between the Mawson and Mullock Glaciers, Antarctica. NZ Geol. Surv. Bull. 71, 157.

Harrington, H.J., 1947. Explicación de las Hojas Geológicas 33m y 34m Sierras de Curamalal y de la Ventana, Provincia de Buenos Aires. Serv. Nac. Min. Geol. Bol. 61, 46. Buenos Aires.

Harrington, H.J., 1970. Las Sierras Australes de Buenos Aires, República Argentina: Cadena Aulacogénica. Rev. Assoc. Geol. Arg. 25 (2), 151–181.

Harrington, H.J., 1972. Sierras Australes de Buenos Aires. Geología Regional Argentina. Acad. Nac. Cs. Córdoba 1972;, 395–405. Buenos Aires.

Harrington, H.J., 1980. Sierras Australes de la Provincia de Buenos Aires, Segundo Simposio de Geología Regional Argentina. Acad. Nac. Cs 2, 967–983. Córdoba.

Harris, N.B.W., Pearce, J.A., Tindle, A.G., 1986. Geochemical characteristics of collision-zone magmatism. In: Coward, M.P., Ries, A.C. (Eds.), Collision Tectonics, vol. 18. Geol. Soc. Special Publications, pp. 67–81.

Hassanen, M.A., 1997. Post-collision, A-type granites of Homrit Waggat Complex, Egypt: petrological and geochemical constraints on its origin. Precambr. Res. 82, 211–236.

Iñiguez Rodríguez, A.M., Andreis, R.R., 1971. Caracteres sedimentológicos de la Formación Bonete, Sierras Australes de la Provincia de Buenos Aires. Reunión Geol. Sierras Australes Bonaerenses. Prov. Buenos Aires, Com. Investig. Científicas 1971;, 103–120. La Plata.

Jackson, N.J., Walsh, J.N., Pegram, E., 1984. Geology, geochemistry and petrogenesis of late Precambrian granitoids in the Central Hijaz region of the Arabian Shield. Contrib. Mineral. Petrol. 87, 205–219.

Keidel, J., 1916. La geología de las sierras de la Provincia de Buenos Aires y sus relaciones con las montañas de Sud-Africa y los Andes. Anales del Ministerio de Agricultura de la Nación. Dir. Geol., Mineral. Min. 9 (3), 1–78.

Kilmurray, J.O., 1968a. Petrología de las rocas cataclásticas y el skarn del anticlinal del Cerro Pan de Azúcar (Partido de Saavedra, Provincia de Buenos Aires). Terceras J. Geol. Arg. Acta Lilloaillana 6, 217–238.

Kilmurray, J.O., 1968b. Petrología de las rocas ígneas de las Sierras Australes de la Prov. de Bs. As. Rev. Museo de La Plata 6 (45), 155–188.

Kilmurray, J.O., 1975. Las Sierras Australes de la Provincia de Buenos Aires, las facies de deformación y nueva interpretación estratigráfica. Rev. Assoc. Geol. Arg. 30 (4), 331–348.

Kilmurray, J.O., Leguizamón, M.A., Teruggi, M.E., 1985. Caracteres estructurales y petrológicos de la Formación Trocadero en las abras de Agua Blanca, abra de Hinojo y Sofia, Sierras Australes de la provincia de Buenos Aires I. J. Geol. Bonaerenses 1985;, 228.

Köhn, J., Ghidella, M., Gianibelli, J., 2002. Integración digital de datos magnéticos en la Provincia de Buenos Aires, Argentina. XV Congr. Geol. Arg. 76–81, El Calafate.

Kostadinoff, J., Prozzi, C., 1998. Cuenca de Claromecó. Rev. Assoc. Geol. Arg. 53 (4), 461–468.

Leat, P.T., Jackson, S.E., Thorpe, R.S., Stillman, C.J., 1986. Geochemistry of bimodal basalt-subalkaline/peralkaline rhyolite provinces within the Southern British Caledonides. J. Geol. Soc. London 143, 259–273.

Llambías, J.E., Prozzi, C.R., 1975. Ventania. Relatorio VI° Congr. Geol. Arg., 79–102, Buenos Aires.

Mattauer, M., Matte, Ph., Malavielle, J., Tapponnier, P., Maluski, H., Qin, X.Z., Lun, L.Y., Qin, T.Y., 1985. Tectonics of the Qinling Belt: build-up and evolution of eastern Asia. Nature 317, 496–500.

Miller, R.B., Paterson, S.R., 1994. The transition from magmatic to high-temperature solid-state deformation: implications from the Mount Stuart batholith, Washington. J. Struct. Geol. 16, 853–865.

Moyes, A.B., Barton Jr., J.M., Groenewald, P.B., 1993. Late Proterozoic to Early Paleozoic tectonism in Dronning Maud Land, Antarctica: supercontinental fragmentation and amalgamation. J. Geol. Soc. Lond. 150, 833–842.

Mullen, E.D., 1983. $MnO/TiO_2/P_2O_5$: a minor element discriminant for basaltic rocks of oceanic environments and its implications for petrogenesis. Earth Planet. Sci. Lett. 62, 53–62.

Paterson, S.R., Vernon, R.H., Tobisch, O.T., 1989. A review of criteria for the identification of magmatic and tectonic foliations in granitoids. J. Struct. Geol. 11 (3), 349–363.

Pearce, J.A., 1982. Trace element characteristics of lavas from destructive plate boundaries. In: Thorpe, R.S. (Ed.), Andesites: Orogenic Andesites and Related Rocks. Wiley, Chichester, pp. 525–548.

Pearce, J.A., Cann, J.R., 1973. Tectonic setting of basic volcanic rocks determined using trace element analyses. Earth Planet. Sci. Lett. 19, 290–300.

Pearce, J.A., Harris, N.B.W., Tindle, A.G., 1984. Trace element discrimination diagrams for the tectonic interpretation of granitic rocks. J. Petrol. 25, 956–983.

Pecerrillo, A., Taylor, S.R., 1976. Geochemistry of Eocene calcoalkaline volcanic rocks from the Kastamonu Area, northern Turkey. Contrib. Mineral. Petrol. 58, 63–81.

Rapela, C.W., Pankhurst, R.J., 2002. Eventos tecto-magmáticos del Paleozoico inferior en el margen Proto-Atlántico del Sur de Sudamérica. XV Congr. Geol. Arg. Actas 2002;, 24–29.

Rapela, C.W., Pankhurst, R.J., Fanning, C.M., Grecco, L.E., 2003. Basement evolution of the Sierra de la Ventana Fold Belt: new evidence for Cambrian continental rifting along the southern margin of Gondwana. J. Geol. Soc. Lond. 160, 613–628.

Rozendaal, A., Gresse, P.G., Scheepers, R., Le Roux, J.P., 1999. Neoproterozoic to Early Cambrian crustal evolution of the Pan-African Saldania belt, South Africa. Precambrian Res. 97 (3/4), 303–323.

Scheepers, R., 1995. Geology and petrogenesis of the Late Precambrian S-, I-, and A-type granitoids in the Saldania belt, Western Cape Province, South Africa. J. African Earth Sci. 21, 35–58.

Scheepers, R., Poujol, M., 2002. Single zircon age of Cape granites suite ignimbrites: characteristics of the last phases of the Saldania magmatism. South African J. Geol. 105, 209–224.

Schiller, W., 1930. Investigaciones Geológicas en las montañas del Sudoeste de la Provincia de Buenos Aires. Anales del Museo de la Plata. Sección Mineral. Geol. Segunda Serie (primera parte) 4, 9–101. La Plata.

Sellés Martínez, J., 1989. The structure of Sierras Australes (Buenos Aires, Argentina). An example of folding in a transpressive environment. J. South Am. Earth Sci. 2 (4), 317–329.

Shand, S.J., 1943. Eruptive Rocks: Their Genesis, Composition, Classification, and Their Relations to Ore-Deposits. Wiley, New York p. 444.

Simpson, C., 1985. Deformation of granitic rocks across the ductile–brittle transition. J. Struct. Geol. 7, 503–511.

Tribe, I.R., D'Lemos, R.S., 1996. Significance of a hiatus in down-temperature fabric development within syn-tectonic quartz diorite complexes, Channel Islands, UK. J. Geol. Soc. Lond. 153, 127–138.

Varela, R., 1973. Edad Rb/Sr de las rocas ígneas de La Mascota-La Ermita, partido de Saavedra, Provincia de Buenos Aires. Anal. Soc. Científica Arg. CXCVI-II1973;, 71–80.

Varela, R., 1978. Sierras Australes de la Provincia de Buenos Aires: Hipótesis de trabajo sobre su composición geológica y rasgos geotectónicos salientes. Rev. Assoc. Geol. Arg. 33 (1), 52–62.

Varela, R., Cingolani, C., 1975. Nuevas edades radimétricas del basamento aflorante en el Perfil del Cerro Pan de Azúcar-Cerro del Corral y consideraciones sobre la evolución geocronoIógica de las rocas ígneas de las Sierras Australes, Provincia de Buenos Aires. VI Cong. Geol. Arg. Actas I, 543–556. Buenos Aires.

Varela, R., Dalla Salda, L.H., Cingolani, C.A., 1985. Estructura y composición geológica de las sierras Colorada, Chasicó y Cortapié, Sierras Australes de Buenos Aires. Rev. Assoc. Geol. Arg. 40 (3/4), 254–261.

Varela, R., Cingolani, C.A., Dalla Salda, L.H., 1990. Edad del granito del Cerro Colorado y su implicancia geotectónica. Sierras Australes de Buenos Aires. XI Congr. Geol. Arg. Actas II II, 279–282. Buenos Aires.

von Gosen, W., 2002. Polyphase structural evolution in the northeastern segment of the North Patagonian Massif (Southern Argentina). J. South Am. Earth Sci. 15, 591–623.

von Gosen, W., Buggisch, W., Dimieri, L., 1990. Structural and metamorphic evolution of Sierras Australes (Buenos Aires Province, Argentina). Geol. Rundschau 79/3, 797–821.

von Gosen, W., Buggisch, W., Krumm, S., 1991. Metamorphic and deformation mechanisms in the Sierras Australes fold thrust belt (Buenos Aires Province, Argentina). Tectonophysics 185, 335–356.

Whalen, J.B., Currie, K.L., Chappell, B.W., 1987. A-type granites: geochemical characteristics, discrimination and petrogenesis. Contrib. Mineral. Petrol. 95, 407–419.

Winchester, J.A., Floyd, P.A., 1977. Geochemical discrimination of different magma series and their differentiation products using immobile elements. Chem. Geol. 20, 325–343.